International Journal of Engineering Research & Technology (IJERT)
ISSN: 2278-0181
Vol. 2 Issue 10, October - 2013

Performance Evaluation of SV PWM Technique for 7-Phase VSI

G.Renukadevi [1] and K. Rajambal [2]

1. Assistant Professor, Dept.of EEE, Jeppiaar Institute of Technology, Sriperumbudur, Chennai
2. Professor, Dept.of EEE, Pondicherry Engineering College, Pondicherry

Abstract

This paper presents the performance evaluation SVPWM technique for 7-phase voltage source inverter in matlab/simulink environment. Seven-phase voltage source inverters are dominantly used to supply the seven-phase drives which are used for high power applications. It is necessary to develop appropriate space vectors for the inverters to provide required output voltages to a seven phase machine. The performances 7-phase VSI are analyzed for MSV, LMSV and LSV techniques. The output voltage and THD are observed through simulation. The performances of the inverter with the above switching vectors are compared for different modulation indices and the results are presented.

Keywords

Large space vectors (LSV), large and medium space vectors (LMSV), medium space vectors (MSV), voltage source inverter(VSI)

I. INTRODUCTION

Multi-phase VSI are becoming as a front end converter for multi-phase drive applications, such as ship propulsion, electric aircraft, and electric/hybrid electric vehicles etc. The multi-phase inverter circuit topology uses two switches connected in series as one inverter pole. The number of inverter poles depends on number of phases. For example, a three-phase inverter will have three inverter arms whereas a nine-phase inverter will have nine inverter arms. Conventional PWM technique adapted for conventional three phase VSI which can be extended for multi-phase VSI also.The most widely used PWM techniques for multi-phase inverters are the carrier-based SPWM and SVPWM [1-15]. The SPWM technique is simple, easy to implement and extensively reported in the literature [1]. However the limitation of SPWM is that the maximum peak of the fundamental component in the output voltage is 50% of the DC link voltage is discussed in [1]. The Carrier-based methods for five-phase VSIs were analyzed in [8-11]. By extending the well-known third harmonic injection principle for three-phase VSIs [8], it has been shown that in the case of a five-phase VSI injection of the fifth harmonic leads to an increase in the DC bus utilization in the linear modulation region is 5.15%. A simplified SVPWM approach is developed in [10-14] by using the concept of offset time. However, SVPWM has become the most popular one because of the easiness of digital implementation and better output voltage compared to sinusoidal PWM method. Moreover, imaginary switching times based SVPWM algorithm is used in [14]. In this method dc bus utilisation is less compared to conventional SVPWM. SVPWM for three-phase voltage source inverter has been extensively discussed in the literature [4]. As far as space vector modulation of a five-phase VSI is concerned, there are a very few SVPWM schemes currently available. The simplest method of realising SVPWM is to utilise only ten large vectors, belonging to the largest decagon in the *d-q* plane, in order to implement the symmetrical SVPWM [15-18]. It is seen that two active space vectors and two zero space vectors are utilised in one switching period to synthesise the input reference voltage. This method is a simple extension of space vector modulation of three-phase VSIs. The only attempt to realise sinusoidal output voltages by means of SVPWM of a five-phase VSI is described in [19,20]. The space vector PWM based seven phase voltage source inverter is considered only in [21, 22]. However, in this scheme six active and two null vectors are considered.

In this paper the performance evaluation SVPWM technique for seven-phase voltage source inverter in matlab/simulink environment is developed. SVPWM technique of a large, medium and combinations of large and medium space vectors are detailed. An attempt is made in this paper for various simulation results are obtained for seven-phase inverter at different modulation indices. The effectiveness of this method is investigated in terms of percentage increase of fundamental voltage and THD for different space vector combinations.

II. POWER CIRCUIT OF SEVEN-PHASE VOLTAGE SOURCE INVERTER

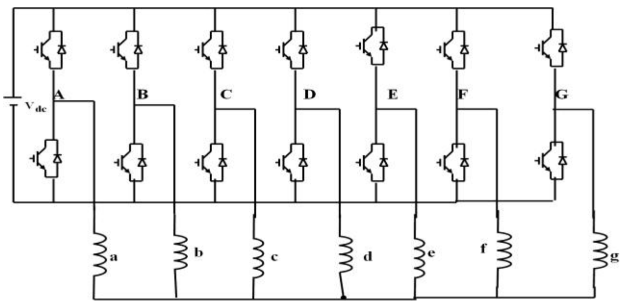

Fig.1 Power circuit diagram of seven-phase VSI

The power circuit of a seven-phase VSI is shown in Fig.1. The circuit consists of *7* half-bridges, which are mutually displaced by $2\pi/n$ degrees to generate the 7-phase voltage waves. The input dc supply is obtained from a single phase or 3-phase utility power supply through a diode-bridge rectifier. The voltages $V_a, V_b, V_c, V_d, V_e, V_f$ *and* V_g are the inverter pole voltages connected to load terminals. It is seen that the switching states of each pole should be combined with each other pole to create the required *7*-phase output voltages. The load phase voltages and inverter pole voltages is as given in the following relations

$$
\begin{aligned}
V_{aN} &= \frac{n-1}{n}V_a - \frac{1}{n}(V_b + V_c + V_d + V_e + V_f + V_g) \\
V_{bN} &= \frac{n-1}{n}V_b - \frac{1}{n}(V_a + V_c + V_d + V_e + V_f + V_g) \\
V_{cN} &= \frac{n-1}{n}V_c - \frac{1}{n}(V_a + V_b + V_d + V_e + V_f + V_g) \\
V_{dN} &= \frac{n-1}{n}V_d - \frac{1}{n}(V_a + V_b + V_c + V_e + V_f + V_g) \\
V_{eN} &= \frac{n-1}{n}V_e - \frac{1}{n}(V_a + V_b + V_c + V_d + V_f + V_g) \\
V_{fN} &= \frac{n-1}{n}V_f - \frac{1}{n}(V_a + V_b + V_c + V_d + V_e + V_g) \\
V_{gN} &= \frac{n-1}{n}V_g - \frac{1}{n}(V_a + V_b + V_c + V_d + V_e + V_f)
\end{aligned} \quad (1)
$$

$$M = \frac{v}{0.5v_{dc}} \quad (2)$$

The svpwm technique for seven phase VSI is discussed detail in the following sections.

III. SVPWM TECHNIQUE

In a seven phase system the inverter space vectors are seven-dimensional space. A space can be decomposed into three two-dimensional sub-spaces (d_1-q_1, d_2-q_2 and d_3-q_3) and one single dimensional sub space (zero-sequence). The problems in the d_2-q_2, d_3-q_3 and zero sub-spaces are extensively reported in [15]. Therefore, in order to generate pure sinusoidal output voltages, SVPWM technique must synthesize fundamental component in the d_1-q_1 plane. In the proposed work, only the d_1-q_1 plane for different space vector is considered. Fig.2 shows the d_1-q_1 plane for seven-phase VSI. In a seven-phase system the inverter space vectors are two-dimensional space as expressed in (3).

$$Vref = \sqrt{\frac{2}{7}}\begin{bmatrix} 1 & \cos\alpha & \cos 2\alpha & \cos 3\alpha & \cos 4\alpha & \cos 5\alpha & \cos 6\alpha \\ 0 & \sin\alpha & \sin 2\alpha & \sin 3\alpha & \sin 4\alpha & \sin 5\alpha & \sin 6\alpha \end{bmatrix} \quad (3)$$

where α=2*pi/n

Thus d_1-q_1 plane can be visualized as being composed of three different space vectors, each plane can be divided into 14 sectors. In the proposed work, a large (outer-most) space vector is considered. This is the simplest extension of a three-phase SVPWM and only the outer most plane is considered in order to generate output voltages, based on the reference space vector. The three types of space vector techniques are detailed in the following subsections.

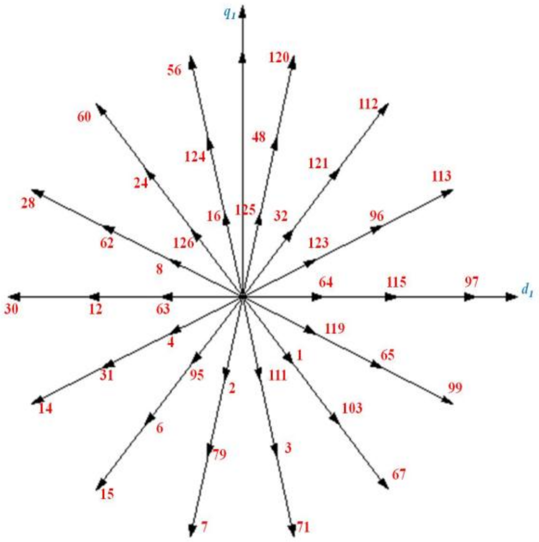

Fig.2. d_1-q_1 plane of seven-phase VSI

a) SVPWM using medium space vectors

The SVPWM scheme discussed in this section considers the medium decagon of space vectors in d_1-q_1 plane. The input reference voltage vector is synthesised from two active neighbouring and zero space vectors. The switching times are calculated by using the reference space vector $V_{ref,}$ magnitude of the medium plane and sector *(sec)* number respectively. The switching time sequence of active and zero space voltage vectors are derived from the expressions (4) & (5).

$$
\begin{aligned}
t_{am} &= \frac{|\bar{V}_{ref}|\sin(\sec\pi/7-\theta)}{|\bar{V}_m|\sin\pi/7}t_s \\
t_{bm} &= \frac{|\bar{V}_{ref}|\sin(\theta-(\sec-1)\pi/7)}{|\bar{V}_m|\sin\pi/7}t_s
\end{aligned} \quad (4)
$$

$$t_0 = t_s - t_{am} - t_{bm} \quad (5)$$

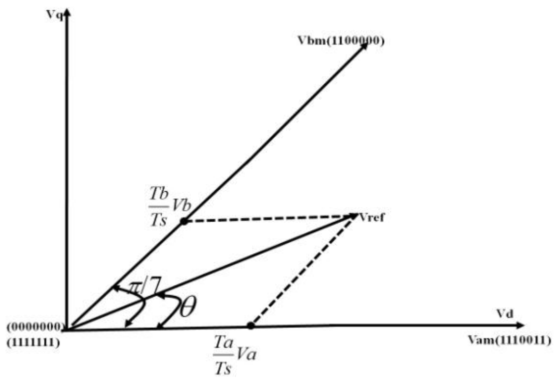

Fig.3 Phasor diagram of Medium space vector

Fig.3 shows the phasor diagram of medium space vector of seven-phase VSI. Here, t_{am} and t_{bm} correspond to times of application of medium space vectors where each sector starts with V_{am} and ends with V_{bm}, respectively. Thus, in sector 1, t_{am} is the time of application of the medium space vector V_{115}, while t_{bm} is the time of application of the medium space vector V_{96}. Total time of application of zero space vectors (equally shared by zero space vectors t_0 and t_{127}) . In odd sectors, sequence of the space vectors over the switching period is (t_0 t_{bm} t_{am} t_{127} t_{am} t_{bm} t_0) , while in even sectors it is (t_0 t_{am} t_{bm} t_{127} t_{bm} t_{am} t_0) respectively. The maximum peak fundamental phase voltage of medium space vectors is $V_{\max} = 0.4V_{dc}$. The switching time sequence of medium space vector of sector 1 is shown in Fig.4.

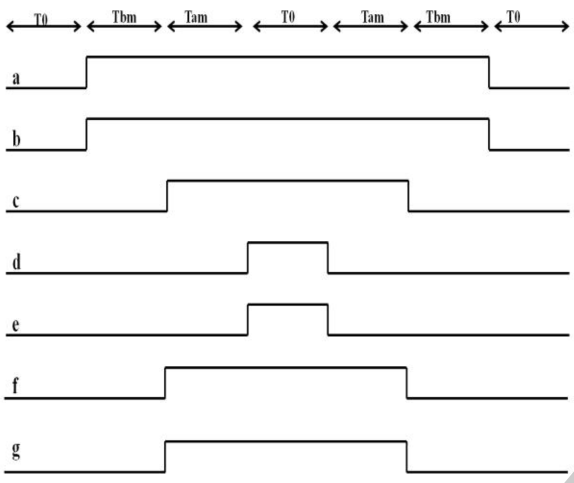

Fig.4 switching time sequence of medium space vectors (sector 1)

b) SVPWM using large and medium space vectors

In the large and medium SVPWM scheme discussed in this section considers the outer and medium decagon of space vectors in d_1 $-q_1$ plane. The switching times are calculated by using the reference space vector $V_{ref,}$ magnitude of the large and medium plane and sector *(sec)* number respectively. The switching time sequence of active and zero space voltage vectors are derived from the expressions (6) & (7).

$$t_a = t_{al} + t_{am}$$
$$t_b = t_{bl} + t_{bm} \tag{6}$$

$$t_{al}\left|\overline{V}_s\right| = t_{am}\left|\overline{V}_m\right|$$
$$t_{bl}\left|\overline{V}_s\right| = t_{bm}\left|\overline{V}_m\right| \tag{7}$$

By solving the system (6) & (7), switching times for active space vectors are obtained as

$$t_{al} = \frac{\left|\overline{V}_l\right|}{\left|\overline{V}_l\right| + \left|\overline{V}_m\right|} t_a \;:\; t_{bl} = \frac{\left|\overline{V}_l\right|}{\left|\overline{V}_l\right| + \left|\overline{V}_m\right|} t_b$$
$$t_{am} = \frac{\left|\overline{V}_m\right|}{\left|\overline{V}_l\right| + \left|\overline{V}_m\right|} t_a \;:\; t_{bm} = \frac{\left|\overline{V}_m\right|}{\left|\overline{V}_l\right| + \left|\overline{V}_m\right|} t_b \tag{8}$$

$$t_0 = t_{al} - t_{bl} - t_{am} - t_{bm} \tag{9}$$

Fig.5 shows the phasor diagram of large and medium space vector of seven-phase VSI. In odd sectors the switching sequence is (t_0 t_{bm} t_{al} t_{bl} t_{am} t_{127} t_{am} t_{bl} t_{al} t_{bm} t_0), while the sequence is (t_0 t_{am} t_{bl} t_{al} t_{bm} t_{127} t_{bm} t_{al} t_{bl} t_{am} t_0) in even sectors. The switching time sequence of large and medium space vector of sector 1 is shown in Fig. 6.

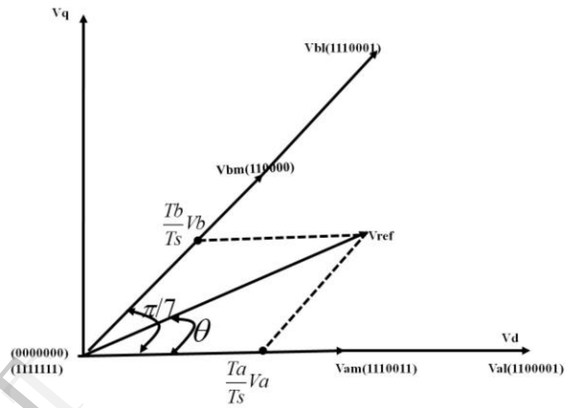

Fig.5 Phasor diagram of large and medium space vector

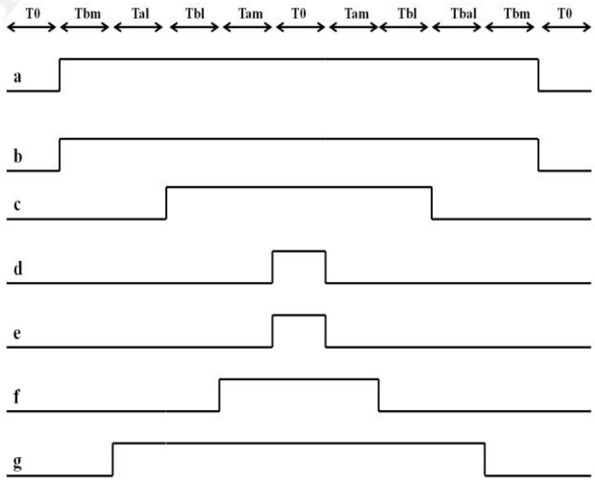

Fig.6 Switching time sequence of large and medium space vectors (sector 1)

c) SVPWM using large space vectors

In this section, the outer-most of large space vectors in d_1 $-q_1$ plane is considered. The input reference voltage vector is synthesised from two active vectors and zero space vectors respectively. The switching times are calculated by using the reference space vector $V_{ref,}$ magnitude of the larger plane and sector *(sec)* number respectively. The switching time sequence of active and zero space voltage vectors are derived from the expressions (10) & (11).

$$t_{al} = \frac{\left|\overline{V}_{ref}\right| \sin(\sec \pi/7 - \theta)}{\left|\overline{V}_{l}\right| \sin \pi/7} t_s \qquad (10)$$

$$t_{bl} = \frac{\left|\overline{V}_{ref}\right| \sin(\theta - (\sec - 1)\pi/7)}{\left|\overline{V}_{l}\right| \sin \pi/7} t_s$$

$$t_0 = 1/2(t_s - t_{al} - t_{bl}) \qquad (11)$$

Fig.7 shows the phasor diagram for large space vectors of seven-phase VSI. Here, t_{al} and t_{bl} correspond to times of application of large space vectors. In sector 1, t_{al} is the time of application of the voltage space vector V_{97}, while t_{bl} is the time of application of the voltage space vector V_{113}. t_0 and t_{127} is the time of application of zero voltage vectors of V_0 and V_{127}. For odd sectors, the sequence of the switching period is $(t_0\ t_{al}\ t_{bl}\ t_{127}\ t_{bl}\ t_{al}\ t_0)$, while in even sectors it is $(t_0\ t_{bl}\ t_{al}\ t_{127}\ t_{al}\ t_{bl}\ t_0)$ respectively. The maximum possible fundamental peak voltage of large space vector is $V_{max}=0.642V_{dc}$. The switching time sequence for large space vectors of sector 1 is shown in Fig.8.

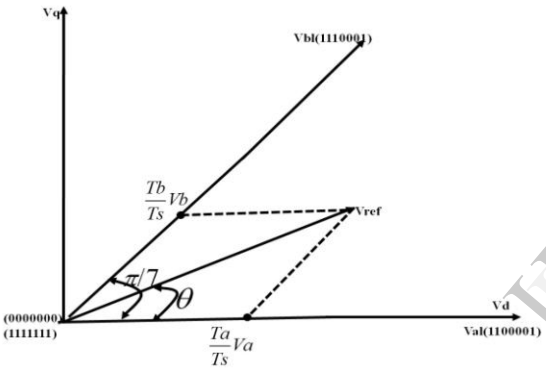

Fig.7 Phasor diagram of large space vector

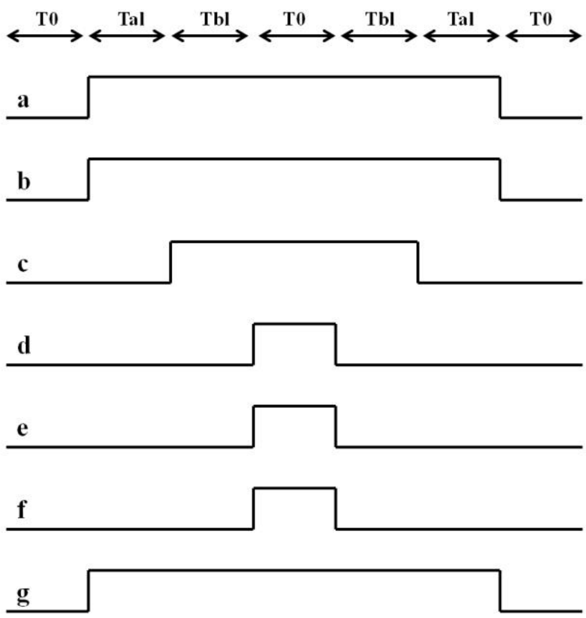

Fig.8 Switching time sequence of large space vectors (sector 1)

IV. SIMULATION RESULTS

A simulation is performed in order to prove the efficiency of the schemes is compared in terms of percentage increase of fundamental voltage and THD. In the simulation the dc link voltage is set to 1 p.u. and the modulation index M is varying from 0.2 to 1. The switching frequency of the VSI is chosen as 10 kHz and the reference fundamental frequency is kept equal to 50 Hz. Fig.9 to Fig.14 shows the simulation results of MSV, LMSV and LSV for 7-phase VSI. Fig.9 shows the resultant modulating waveform for medium space vectors. Fig.10 shows the phase voltage and its spectrum of medium space vector. From the observation the fundamental rms value equals 0.3589 (0.5075 peak) and THD is 75.16%. The large and medium space vector modulating signals and output phase voltage is shown in Fig.11 and 12. It is seen that the fundamental rms value equals 0.4215 (0.5961 peak) and THD is 54.65% respectively. The large space vector modulating signals and output voltage is shown in Fig.13 and 14. It is seen that the fundamental rms value equals 0.4474 (0.6328 peak) and THD is 46.57% respectively. The deviation of the percentage decrease of THD versus different space vectors is shown in Table.1and it is projected in Fig.15.

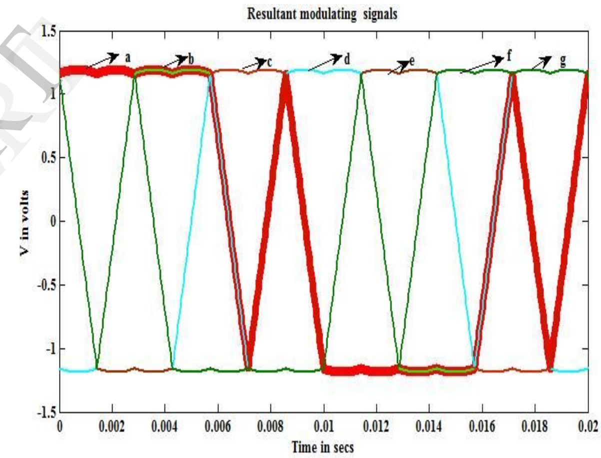

Fig.9. Resultant modulating signal for medium space vectors

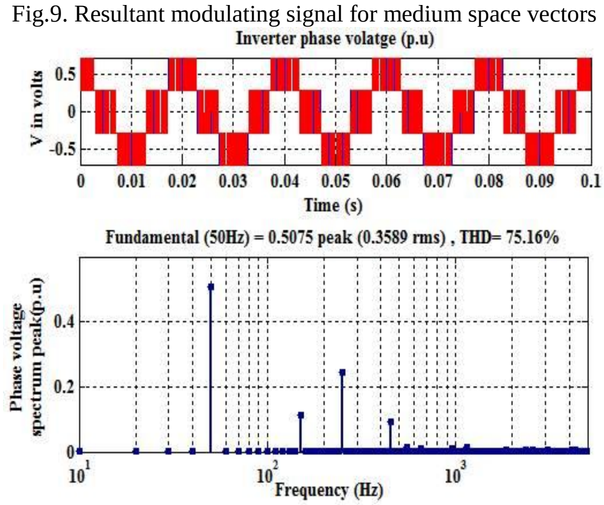

Fig.10. output phase voltage and its spectrum of medium space vectors when $M = 0.85$

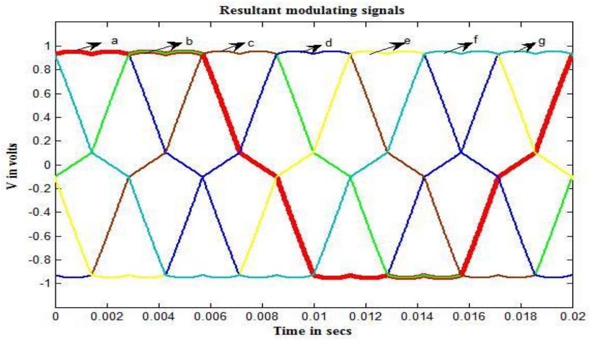

Fig.11. Resultant modulating signal for large and medium space vectors

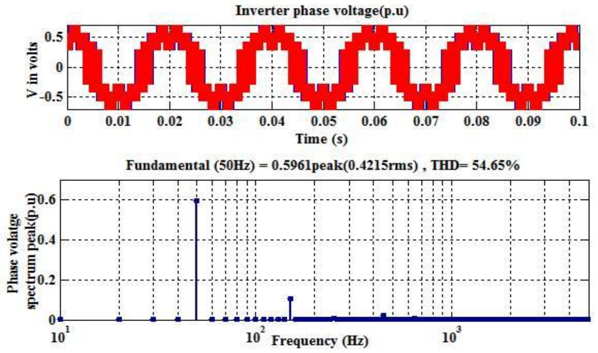

Fig.12. output phase voltage and its spectrum of large and medium space vectors when $M = 0.85$

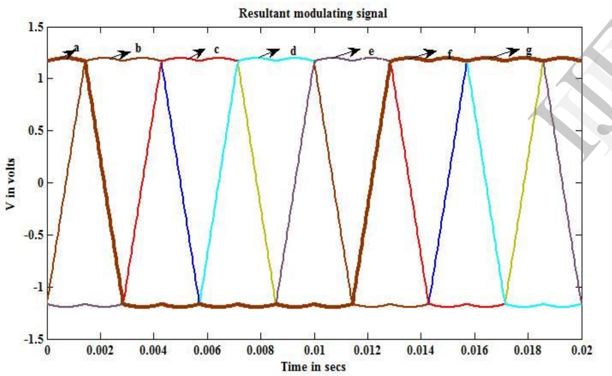

Fig.13. Resultant modulating signal for large space vectors

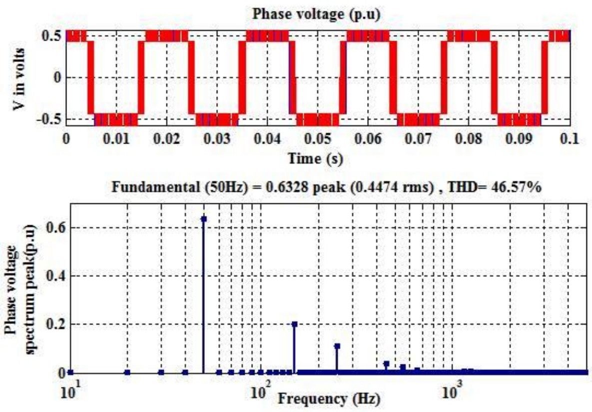

Fig.14. output phase voltage and its spectrum of large space vectors when $M = 0.85$

Table I
Comparison of % THD for various SVPWM techniques

MI	Medium space vectors THD%	Large & Medium space vectors THD%	Large space vectors THD%
0.2	199.02	181.93	**169.75**
0.4	126.52	110.16	**100.66**
0.6	87.12	69.71	**61.94**
0.85	75.16	54.65	**46.57**

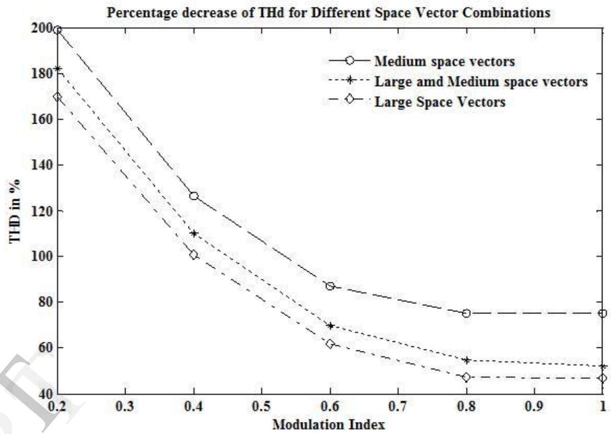

Fig.15. Percentage decrease of THD for different space vectors combinations

V. CONCLUSION

A simulation study of a seven-phase VSI with three different space vector switching technique is presented in this paper. From the simulation results, it is seen that the large, medium space vector technique involves two active vectors whereas large and medium as four active vectors, thus increasing the complexity in the LMSV switching scheme. The THD is observed to be 75.16%, 54.65% and 46.57% for MSV, combination of LMSV and LSV at the rated modulation index of 0.85. The THD increases with decreasing modulation index and it is minimum for large space vectors. Based on the THD, fundamental voltage and switching pattern and space vector disposition complexity the large space vectors is optimum for seven-phase voltage source inverter.

REFERENCES

[1] G.K.Singh,“Multi-phase induction machine drive research – a survey,*electric Power System Research*, vol. 61, pp. 139-147,2002.

[2] G.Renukadevi and K.Rajambal, “Generalized Model of Multi-Phase Induction Motor Drive using Matlab/Simulink,” *International IEEE PES Conference Innovative Smart Grid Technologies*,Kerala-India, 2011.

[3] E.Levi,R.Bojoi,F.Profumo,H.A.Toliyat and S. williamson, “Multiphase induction motor drives-A technology status

review",*IET Elect. Power Appl.* vol. 1, no. 4, pp. 489-516, July 2007.

[4] G.D.Holmes, T.A.Lipo, "*Pulse Width Modulation for Power Converters -Principles and Practice,*" IEEE Press Series on Power Engineering, John Wiley and Sons, Piscataway, NJ, USA, 2003.

[5] Y.Zhao, T.A.Lipo. Space vector PWM control of dual three-phase induction machine using vector space decomposition, IEEE Trans. on Industry Applications, vol. 31, no. 5, 1995, pp. 1 100-1 109.

[6] R.O.C.Lyra, T.A.Lipo, "Torque density improvement in a sixphase induction motor with third harmonic current injection,"*IEEE Trans. on Industry Applications,* vol. 38, no. 5, 2002, pp.1351-1360.

[7] H.M.Ryu, J.H.Kim, S.K.Sul, "Analysis of multi-phase space vector pulse width modulation based on multiple d-q spaces concept," *IEEE Trans. on Power Electronics,* vol. 20, no. 6, 2005, 1364-1371.

[8] S. Xue, X. Wen, Z. Feng, "A novel multi-dimensional SVPWM strategy of multiphase motor drives," *Proc. Power Electronics and Motion Control Conf. EPE-PEMC,* pp. 931-935, 2006.

[9] E.Levi, "Multiphase Electric Machines for Variable Speed Applications," *IEEE Transactions on Industrial Electronics,* vol. 55, no. 5, pp. 1893-1909, MAY 2008.

[10] A.Iqbal, E.Levi, M.Jones, S.N.Vukosavic, "Generalised sinusoidal PWM with harmonic injection for multi-phase VSIs," *Proc. IEEE Power Elec. Spec. Conf., PESC,* Jeju, Korea, 2006, pp. 2871-2877.

[11] D.Casadei, G.Serra, A.Tani, L.Zarri, "Multi-phase inverter modulation strategies based on duty-cycle space vector approach,"*Proc. of Ship Propulsion and Railway Systems Conf. SPRTS,*Bologna, Italy, 2005, pp. 222-229.

[12] G.Renukadevi and K.Rajambal, "Novel Carrier-Based PWM technique for n-Phase VSI," *International Journal of Energy Technologies and Policy*, 2011, pp. 1-9.

[13] O.Ojo, G.Dong, "Generalized discontinuous carrier-based PWM modulation scheme for multi-phase converter-machine systems," *Proc. IEEE Ind. Appl. Soc. Annual Meeting IAS,* Hong Kong,2005, CD-ROM paper IAS38p3.

[14] Joohn-Sheok Kim and Seung-Ki Sul, "A novel voltage modulation technique of the space vector PWM", in *Conf. Rec. IPEC'95,* Yokohama, Japan, 1995, pp. 742-747.

[15] T.Brahmananda Reddy, J. Amarnath and D. Subbarayudu,"Improvement of DTC performance by using hybrid space vector Pulsewidth modulation algorithm" *International Review of Electrical Engineering*, Vol.4, no.2, pp. 593-600,Jul-Aug, 2007.

[16] Kelly, J.W., Strangas, E.G., and Miller, J.M.: 'Multi-phase inverter analysis'. Proc. IEEE Int. Electric Machines and Drives Conf. IEMDC, Cambridge, MA, 2001, pp. 147–155.

[17] R.Shi, H.A.Toliyat, "Vector control of five-phase synchronous reluctance motor with space vector pulse width modulation (SVPWM) for minimum switching losses," *Proc. IEEE Applied Power Elec. Conf. APEC,* Dallas, Texas, 2002, pp. 57-63.

[18] H.A.Toliyat, R.Shi, H.Xu, "DSP-based vector control of five-phase synchronous reluctance motor," *IEEE Industry Applications Society Annual Meeting IAS,* Rome, Italy, 2000, CD-ROM paper no. 40_05.

[19] P.S.N.deSilva, J.E.Fletcher, B.W.Williams, "Development of space vector modulation strategies for five-phase voltage source inverters," *Proc. IEE Power Electronics, Machines and Drives Conf. PEMD,* Edinburgh, UK, 2004, pp. 650-655.

[20] Iqbal and S. Moinuddin, "Space vector model of a five-phase voltage source inverter," in *Proc. IEEE Int. Conf. Ind. Technol. (ICIT 2006),* Mumbai, India, Dec.15–17, pp. 488–493, Paper IF 002909 [CD-ROM].

[21] G. Grandi, G. Serra, and A.Tani, "Space vector modulation of a seven phase voltage source inverter," *International Symposium on Power Electronics*, SPEEDAM 2006.

[22] D.Dujic, E.Levi, M.Jones, "Continuous PWM Techniques for Sinusoidal Voltage Generation with Seven-Phase Voltage Source Inverters," *Proc. IEE Power Electronics, specialist conference* PESC 2007